Design of a Depth of Interaction (DOI) PET Detector Module

R.S. Miyaoka, T.K. Lewellen, H. Yu[1], and D.L. McDaniel[2]

University of Washington and *General Electric Medical Systems

[1]University of Washington Medical Center, Seattle, WA 98195

[2]General Electric Medical Systems, Waukesha, WI 53188

Abstract

A method to determine depth of interaction (DOI) from a PET detector module is described and evaluated. The basic element of the DOI detector module is a two crystal detector unit. The hypothesis is that by controlling how light is shared between two crystals (A and B) DOI information can be extracted from the ratio of light collected using simple Anger logic [(A-B)/(A+B)]. The interface between crystals is designed so that a significant amount of light is shared when a photon interacts near the front face of a crystal and very little light is shared when an interaction occurs near the back of a crystal. The effects of surface treatment (e.g., polished, roughened) and optical coupling compounds are investigated. BGO, GSO and LSO detector units have been evaluated. A DOI uncertainty of ~6mm was attained for the front section (~4mm) of a 2x2x20mm LSO detector unit. A method to decode a 64 crystal detector module (32 detector units) using a 16 channel multi-anode photomultiplier tube is described.

I. INTRODUCTION

Degradation in spatial resolution for sources distant from the center of the field of view (FOV) is characteristic of all ring based PET detector systems. This non-symmetric broadening of the point source profile is a result of assigning detected events to the wrong line of response (LOR), see Figure 1 (solid-correct; dashed-misplaced). The spatial broadening is primarily a function of crystal length and the angle of incidence of the photons. Therefore as the intrinsic spatial resolution of PET systems improves, one must either sacrifice resolution uniformity or detection sensitivity (i.e., use shorter detectors). A detector system that provides depth of interaction (DOI) information can correctly position these events resulting in more uniform resolution throughout the FOV. DOI information can also enhance the performance of a PET detector system by improving the sampling characteristics of the detector system and allowing the use of smaller ring diameters to increase coincidence sensitivity.

A number of methods to extract DOI information from a PET detector module have been proposed [1-8]; however, no current PET system provides DOI information. A drawback to a number of the proposed methods is the requirement of additional detector electronics (i.e., photodiodes or additional photomultiplier tubes (PMTs)). With the discovery of LSO [9] and the improvement in the manufacturing of GSO[10]) there has been renewed interest in development of DOI detector system.

Current generation PET block detectors optimize the way light is shared throughout the module for crystal identification

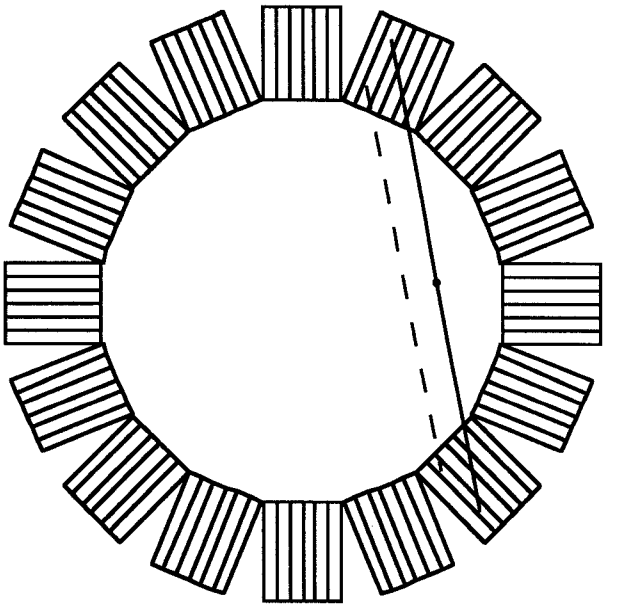

Figure 1. Line of response (dashed line) misplace due to DOI effect.

[11]. Using simple Anger logic [12] modules with up to 64 crystals have been decoded using 4 PMTs [11]. Instead of using the light to decode as many crystals as possible, this work investigates methods to share light to extract DOI information. The hypothesis is that by controlling how light is shared between neighboring crystals (A and B) DOI information can be extracted from the ratio of light collected using simple Anger logic [(A-B)/(A+B)]. The interface between crystals will be designed so that a significant amount of light is shared when a photon interacts near the front face of a crystal and very little light is shared when an interaction occurs near the back of a crystal (see Figure 2). Furthermore, the interface will be designed so the front section of the detector (where most of the interactions will occur) is more sensitive to DOI effects than the back section of the detector unit. For this investigation a detector unit consists of two optically coupled crystals.

II. EXPERIMENTAL METHODS

BGO, GSO and LSO detector units were built and evaluated. The dimensions and surface finishes of the crystals used are listed in Table 1. Each of the four detector units tested are illustrated in Figures 3-5. Each detector unit was coupled to a 16 channel (4x4) metal dynode PMT (R6568, Hamamatsu Corp., Japan) for testing. The LSO crystals were

0-7803-4258-5/98/$10.00 © 1998 IEEE

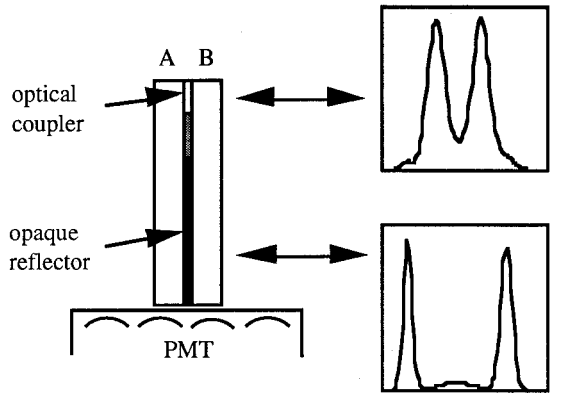

Figure 2. DOI decoding strategy.

Table 1.
Dimensions and surface finish of crystals.

Crystal	Dimensions (mm)	Surface Finish
BGO	3.9 x 4.1 x 30	polished
GSO #1	3.9 x 4.1 x 30	unpolished
GSO #2	2.6 x 3.5 x 24*	3.5 x 24 unpolished 2.6 x 24 polished
LSO	2.0 x 2.0 x 20*	polished

* two 12 mm crystals glued together
** two 10 mm crystals glued together

coupled to the PMT via 2mm diameter by 7.5cm long double clad optic fibers (Kurraray, Japan). The BGO and GSO crystals were directly coupled to the PMT. A high index of refraction, 1.74, resin (Cargille, New Jersey) was used to facilitate light sharing between crystals. The same resin was used to glue the individual sections of GSO detector unit #2 and the LSO detector unit. For the crystals with polished surfaces, the section of the interface coupled with the resin was roughened to enhance light sharing. Detector units were evaluated using both white latex paint and TFE Teflon as the opaque reflective material along the crystal interface. After the crystal interface was completed the detector units were wrapped in TFE Teflon and coupled to the PMT.

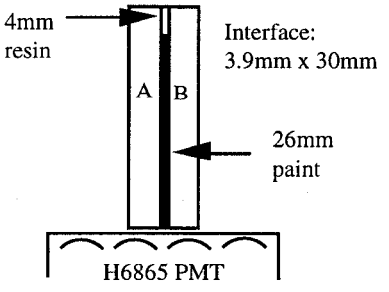

Figure 3. Detector design for GSO detector unit #1 and BGO detector unit.

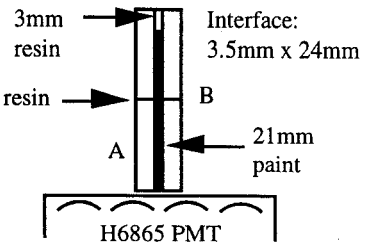

Figure 4. Detector interface for GSO detector unit #2. Two 2.6 x 3.5 x 12mm crystals are glued together to form crystals A and B.

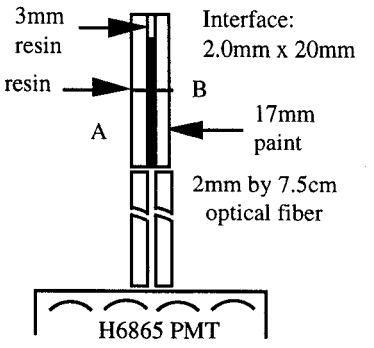

Figure 5. Detector interface for LSO detector unit. Two 2.0 x 2.0 x 10mm crystals are glued together to form crystals A and B.

A block diagram of the acquisition setup is illustrated in Figure 6. The detector unit was exposed to a narrow flux (~3mm) of 511 keV photons (flux perpendicular to long axis of crystals) using a shielded ^{68}Ge line source. The photon flux was stepped along the length of the detector unit in ~3mm increments. Only signals from the two channels directly coupled to the detector unit were acquired. The FERA ADC (LeCroy, Chestnut Ridge, NY) integration time was 200 ns for LSO, 300 ns for GSO and 775 ns for BGO. A long background acquisition was taken for the LSO detector unit to correct for its natural background activity.

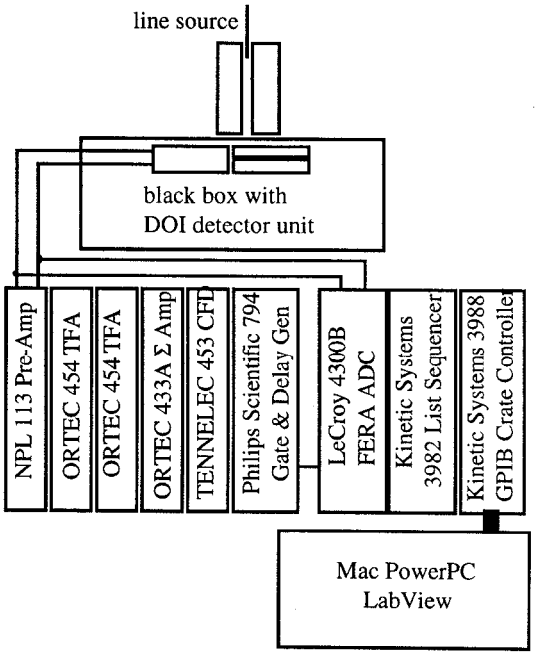

Figure 6. Experimental setup.

III. RESULTS

A subset of the ratio plots for GSO detector unit #1 (DOI positions: 2mm, 8mm and 23mm) are shown in Figure 7. An energy window around the photopeak was applied to the data prior to binning. The lower peak corresponds to interactions in crystal B, while the upper peak corresponds to interactions in crystal A. The position of the ratio peak for each of the depth of interaction (DOI) positions for crystal B is plotted in Figure 8. The positions of the full width at half maximum (FWHM) of the ratio peak were also plotted. The points associated with the FWHM ratio values were each fit with a 3rd order polynomial. Horizontal error bars (shown for depth = 5mm) were used to estimate the DOI uncertainty for positions along the length of the detector unit. A plot of the uncertainty versus DOI position is shown in Figure 10. The uncertainty values plotted have not been corrected for the width (~3mm) of the source. Plots of uncertainty versus DOI for crystal B of GSO detector unit #2 and the LSO detector unit are shown in Figures 11 and 12, respectively. While there was movement in the ratio peaks for the BGO detector unit, using this type of analysis, no DOI information could be extracted (i.e., the uncertainty was 30mm at each DOI position).

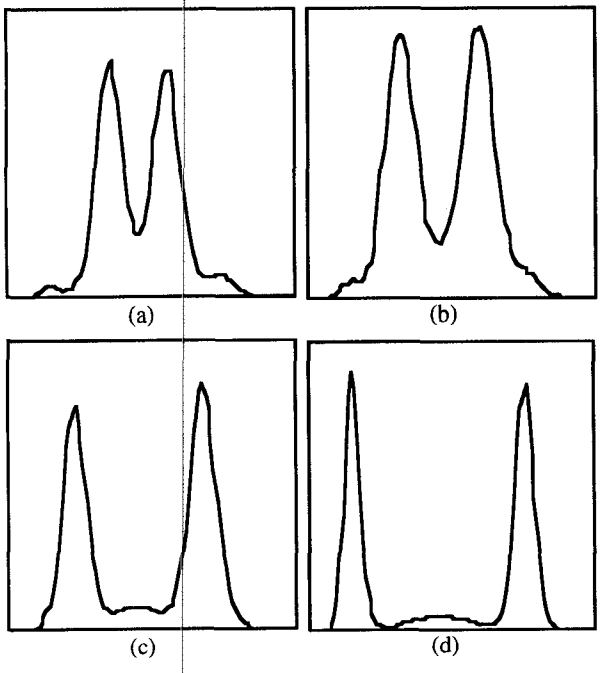

Figure 7. Ratio plots for GSO detector unit #1 at DOI positions 2mm (a), 5mm (b), 11mm (c) and 23mm (d).

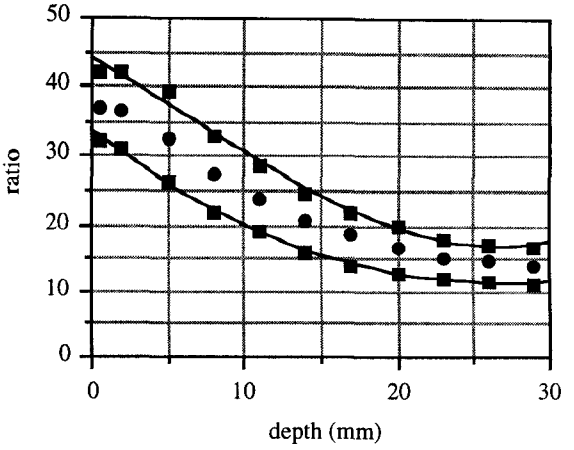

Figure 8. Ratio peak and FWHM values of ratio plot versus DOI for GSO detector unit #1 (crystal B). Horizontal line is estimate of DOI uncertainty for depth position.

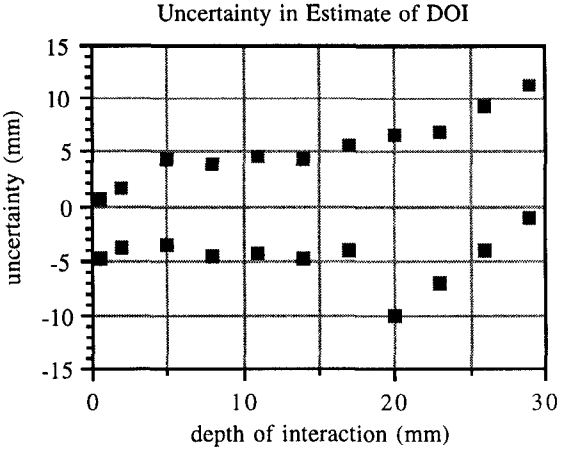

Figure 9. Uncertainty in estimate of DOI for GSO detector unit #1.

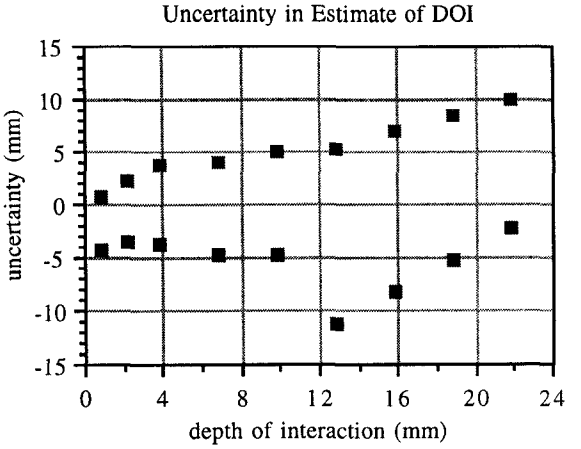

Figure 10. Uncertainty in estimate of DOI for GSO detector unit #2.

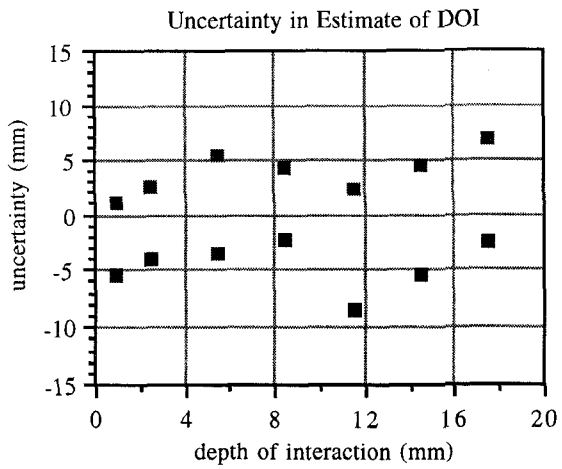

Figure 11. Uncertainty in estimate of DOI for LSO detector unit.

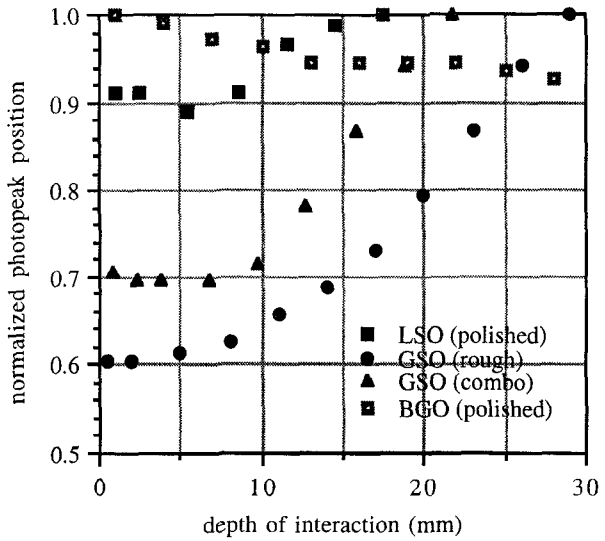

Figure 12. Plot of normalization photopeak position (ADC channel) versus DOI.

The position of the photopeak (energy spectra) also varied with DOI. A plot of the photopeak position versus DOI, individually normalized for each detector unit, is shown in Figure 12.

IV. DISCUSSION

For three of the detector units evaluated a DOI accuracy of ~5mm was attained for the front section of the crystals and better than 10mm accuracy was attained for the front half of the detector units. While there was some movement in the ratio peaks for the BGO detector unit, almost no DOI information was provided.

While GSO crystals produce more light than BGO crystals, the amount of light collected from the front section of the GSO detector unit #1 was only slightly more than the light collected from the BGO module. Additionally, the light collected from the LSO detector unit was approximately equal to the light collected from the BGO detector unit. We believe that the DOI decoding technique worked well for GSO detector unit #1 because light lost at the unpolished surfaces of the GSO crystals makes the collection of light a strong function of the initial direction of the light photons (a requirement to make this technique work). It is unlikely that light photons produced near the rear of the detector unit will survive enough surface interactions (reflections) to make it across the optically coupled region of the crystal. For polished crystals (4x4x30mm), our results indicate that the amount of light shared across the optically coupled interface is not very correlated with where the light originated. While the LSO crystals were polished, the collection of light was still a strong function of the initial direction of the light photons. This is because for very narrow crystals it takes many more reflections for light originating near the rear of the crystal to make it to the optical interface. While we glued crystals together because we did not have crystals that were long enough to evaluate this technique, it (gluing) may have serendipitously improved the DOI decoding performance of the LSO and the GSO #2 detector units.

V. MODULE DESIGN

The decoding strategy for a detector module consisting of 32 detector units (total of 64 crystals); each crystal having a 2mm by 2mm front face is shown in Figure 14 (see next page). Fiber optic connectors are used to route the light from the crystals to the 16 channel metal dynode PMT (H6568-10, Hamamatsu, Japan). Each anode (labeled **1-16**) receives light from 4 crystals. A discrete decoding scheme (Table 2) will be used to determine the detector unit (2 crystals - labeled *a-ff*) of interest. Once a detector unit is selected, Anger logic is used to determine which crystal the event occurred in and to estimate DOI.

Table 2.
Decoding strategy for 64 crystal detector module (32 - detector units).

detector unit	anode pair	detector unit	anode pair	detector unit	anode pair	detector unit	anode pair
a	**1-5**	*i*	**5-9**	*q*	**9-13**	*y*	**13-1**
b	**1-6**	*j*	**6-9**	*r*	**9-14**	*z*	**14-1**
c	**2-6**	*k*	**6-10**	*s*	**10-14**	*aa*	**14-2**
d	**2-7**	*l*	**7-10**	*t*	**10-15**	*bb*	**15-2**
e	**3-7**	*m*	**7-11**	*u*	**11-15**	*cc*	**15-3**
f	**3-8**	*n*	**8-11**	*v*	**11-16**	*dd*	**16-3**
g	**4-8**	*o*	**8-12**	*w*	**12-16**	*ee*	**16-4**
h	**4-5**	*p*	**5-12**	*x*	**12-13**	*ff*	**13-4**

VI. CONCLUSION AND FUTURE DIRECTIONS

Some DOI information can be extracted from a two crystal detector unit. The amount of DOI information is a strong function of surface finish and the crystal dimensions. A DOI uncertainty of ~5mm was attained for the front section of the GSO and LSO detector units evaluated. The uncertainty increased to ~10mm in the center section of the detector units. The uncertainty in the rear of the detector units was limited by the end of the crystal.

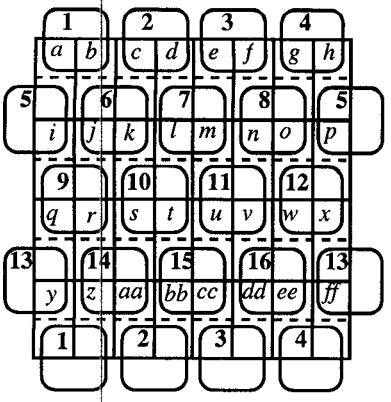

Figure 14. Decoding strategy for 64 crystal detector module (32 - detector units). The numbered squares represent dynode channels of a 16 channel multi-anode PMT (Hamamatsu R6568-10). The rectangles (italic letters) represent detector units. Each detector unit is represented by a unique anode pair. Decoding of the module is illustrated in the Table 2.

The module design described in this paper is proposed for specialized imaging systems (e.g., small animal, breast, dedicated head) and is not practical for whole-body PET systems. On the other hand, a 6x6 module comprised of 4x4x30mm GSO or LSO crystals with DOI capability would very attractive for clinical PET imaging systems. Therefore, we have started to extend this technique to larger detector arrays (e.g., 1x4 and 1x6). Our preliminary findings are promising. Since the DOI determination only has to be done once, extending a 1x6 module into a 6x6 module should be somewhat straightforward.

VII. ACKNOWLEDGMENTS

This work was supported in part by PHS grant CA42593 and General Electric Medical Systems.

The authors would like to thank Dr. Simon Cherry for loaning us the LSO crystals and providing us with some 2mm double clad optical fibers. The authors would also like to thank Mr. Scott Dodson for providing some GSO crystals during the early stages of this work.

VIII. REFERENCES

[1] Derenzo SE, Moses WW, et. al., "Initial Characterization of a Position-Sensitive Photodiode/BGO Detector for PET," *IEEE Trans Nuc Sci.*, vol. 36(1), pp.1084-89, February 1989.

[2] Shimizu K, Ohmura T, Watanabe M, Uchida H, Yamashita T, "Development of 3-D Detector System for Positron CT," *IEEE Trans Nuc Sci.*, vol.35(1), pp.717-20, February, 1988.

[3] Rogers J, et. al., "Design of a Volume-imaging Positron Emission Tomograph", *IEEE Trans Nuc Sci.*, vol.36(1), pp.993-7, February, 1989.

[4] Wong WH, "Designing a Stratified Detection System for PET Cameras," *IEEE Trans Nuc Sci.*, vol.33(1), pp.591-6, February, 1986.

[5] Yamashita T, Watanabe M, Shimizu K, Uchida H, "High Resolution Block Detectors for PET," *IEEE Trans Nuc Sci.*, vol.37(1), February, 1990.

[6] Karp JS, Daube-Witherspoon ME, "Depth-of-Interaction Determination in NaI(Tl) and BGO Scintillation Crystals Using a Temperature Gradient," *Nucl. Instr. Meth.* vol.A260 pp.509-17, October, 1987.

[7] Bartzakos P, Thompson CJ, "A Depth-Encoded PET Detector", *IEEE Trans Nuc Sci.*, vol.38(2), pp.732-8, April, 1991.

[8] Rogers J, "A Method for Correcting the Depth-of-Interaction Blurring in PET Cameras", *IEEE Trans Med Imag.* vol.14(1), pp.146-50, March, 1995.

[9] Melcher CL, Schweitzer JS, "Cerium-doped Lutetium Oxyorthosilicate: A Fast, Efficient New Scintillator," *IEEE Trans Nuc Sci.*, vol.39(4), pp.502-5, August, 1992.

[10] Takagi K, Fukazawa T, "Cerium-activated Gd/sub 2/SiO/sub 5/ single crystal scintillator," *Appl. Phys. Lett.* vol.42(1), pp.43-5, January, 1983.

[11] Tornai MP, Germano G, Hoffman EJ, "Positioning and Energy Response of PET Block Detectors with Different Light Sharing Schemes", *IEEE Trans Nuc Sci.* vol.41(4) pp. 1458-63. Aug. 1994.

[12] Anger HO. Radioisotope Cameras, in Instrumentation in Nuclear Medicine (vol 1) chap 19. Academic Press, 1967.